Recent Climate Change in the Tropical Western Pacific and Indian Ocean Regions as Detected by Outgoing Longwave Radiation Records*

PAO-SHIN CHU AND JIAN-BO WANG

Department of Meteorology, School of Ocean and Earth Science and Technology, University of Hawaii at Manoa, Honolulu, Hawaii

(Manuscript received 3 October 1995, in final form 17 August 1996)

ABSTRACT

Recent climate change in tropical convection in the western Pacific and Indian Ocean regions is inferred from the outgoing longwave radiation (OLR) records. The systematic bias in the OLR series is first corrected and results of the rotated empirical orthogonal function analysis indicate that the bias, to a first approximation, has been corrected.

Linear regression analysis and nonparametric Mann–Kendall rank statistics are employed to detect trends. From 1974 to 1992, trend analyses based on the entire consecutive monthly records suggest a significant decrease in OLR over the tropical central–western Pacific and a large portion of the Indian Ocean. In contrast, northern Australia shows the largest increase in OLR over time. The significance of the local linear trend pattern has been determined via a Monte Carlo simulation technique that scrambles OLR time series at each grid point ''simultaneously'' and results show the field significance.

An increase in convection shows a preference to occur in the summer hemisphere. During the boreal summer half-year, this is seen in a region extending from the Arabian Sea across southeast Asia eastward to the northwest Pacific, with the largest value over the Bay of Bengal. More summer monsoon rainfall is likely to have occurred in these regions. For the austral summer half-year, enhanced convection is found over the equatorial south-central Pacific and the south-central Indian Ocean. Time series of tropical cyclone counts in the northwest Pacific, the Bay of Bengal, and the south-central Indian Ocean also reveal a general level of increase. Regardless of seasonality, a positive trend in OLR is always observed over a large portion of tropical Australia.

A sensitivity test is conducted to investigate the change in linear trend patterns by removing the years during which the El Niño–Southern Oscillation phenomenon occurred. Although the enhanced convection over the Bay of Bengal, the south Indian Ocean, and the northwest Pacific are still noticeable, it is much weaker over the equatorial south-central Pacific than when the complete duration series were used. Other sensitivity tests are also conducted to examine the change in linear trend patterns by varying data lengths and by skipping the missing 10-month observation in the OLR time series; results are basically similar to those when complete data are used. The authors speculate that monsoon convection over the tropical western Pacific and the Indian Ocean has undergone a change in the climate mean state, probably on a decadal timescale.

1. Introduction

The total world population will reach about 6.5 billion by the year 2000. The regions of major increase in population will be composed mainly of countries within the humid Tropics (Gladwell and Bonell 1990). This growth will put an ever increasing demand on water resources for drinking, agriculture, food production, and recreation purposes.

Meteorologically, the most intense heat source regions in the global Tropics, namely, the Bay of Bengal, the South China Sea, and the Indonesian Maritime Continent, are located within the Indian Ocean and western Pacific Ocean sectors (Ding 1994). Heavy convective precipitation and associated release of heat of condensation in these regimes drive a large portion of the general circulation in the global Tropics and midlatitudes (Krishnamurti and Surgi 1987; Lau and Chang 1987). The tropical western Pacific is known as the warm pool region in which sea surface temperatures (SST) remain high throughout the year, and small changes in SST may invoke a large planetary-scale climate response (Palmer and Mansfield 1984).

Because of the important role of the tropical western Pacific and the Indian Ocean in the global climate system, it is desirable to know if there are any observable climate changes over recent years. Information from climate change detection is of interest not only for inferences on the future evolution of the climate but may also be useful in the development of long-term sustain-

* School of Ocean and Earth Science and Technology Contribution Number 4186.

Corresponding author address: Dr. Pao-Shin Chu, Department of Meteorology, School of Ocean and Earth Science and Technology, University of Hawaii at Manoa, 2525 Correa Road HIG 331, Honolulu, HI 96822.

© 1997 American Meteorological Society

Brought to you by NATIONAL TAIWAN UNIV | Unauthenticated | Downloaded 10/08/23 02:42 PM UTC

able land-use policies for many countries (e.g., Thailand, Indonesia) located in the study domain.

Nitta and Yamada (1989) used outgoing longwave radiation (OLR) as an index of tropical convective activity to investigate decadal variations of atmospheric circulation in the global tropical belt. Their second eigenmode pattern and the associated time-dependent eigen coefficients of OLR suggest that convective activity in the tropical Indian and central Pacific Oceans was consistently stronger in the 1980s than in the 1970s. However, because of systematic bias in OLR occurring from the differences in equatorial crossing time among satellites not being taken into account, as noted by Gadgil et al. (1992) and Chelliah and Arkin (1992), the findings of Nitta and Yamada are subject to uncertainty and require further investigations.

In this regard, the bias-corrected OLR described in section 2 will be used in this study. The OLR data have been used extensively to study tropical convection and even to make direct estimates of tropical precipitation (e.g., Motell and Weare 1987; Yoo and Carton 1988). Section 3 discusses methods used in trend detection and section 4 provides a measure to assess the success in correcting the artificial satellite biases. Section 5 describes the local and field significance of trend patterns. Section 6 describes the trend analyses, and section 7 discusses the sensitivity tests of linear regression trends. Finally, section 8 gives a summary and discussion.

2. Data and bias correction

The main dataset is the daily averaged OLR. The values of OLR are derived from measurements taken by scanning radiometers or advanced very high resolution radiometers aboard the National Oceanic and Atmospheric Administration (NOAA) polar-orbiting satellites. The OLR represents an integral measure of the radiative effects from the surface, clouds, and gases in the atmosphere. If the sky is clear, the radiometer monitors longwave radiation emitted mainly from the earth's surface. In the case of deep convective clouds, the sensors measure radiation from the top of the clouds. Thus, the satellite-derived OLR in the Tropics primarily reflects cloud-top temperatures, with low OLR values corresponding to cold and high clouds, which denotes enhanced convection. An inverse relationship generally holds between OLR and convection.

The OLR data available to us are at 5° lat/long resolution for more than 18 yr from June 1974 to December 1992 (a gap of 10 months in 1978) between 22.5°N and 22.5°S. In contrast to a small number of rain gauges arrayed at irregular locations over the oceans, OLR data have the advantages of being spatially homogeneous and of common length of observations at each of the grid points. The ground rainfall stations also suffer a host of other problems such as station relocations, instrument changes, changes in the time of observations, different length of observations, missing observations, and many other factors. It is generally difficult to locate or correct for inhomogeneities resulting from these factors for climate change detection study. In fact, space-borne sensors provide the only available means for estimating tropical convection or rainfall or both over the oceans on a regular basis.

TABLE 1. Longwave radiation measurements from NOAA satellites (adapted from Chelliah and Arkin 1992).

Satellite	Local equator crossing times	Period of record	Number of months
NOAA SR series (*NOAA-2, -3, -4, -5*)	0900, 2100 LST	Jun 1974–Feb 1978	45
TIROS-N	0330, 1530 LST	Jan 1979–Jan 1980	13
NOAA-6	0730, 1930 LST	Feb 1980–Aug 1981	18
NOAA-7	0230, 1430 LST	Sep 1981–Feb 1985	41
*NOAA-9**	0230, 1430 LST	Feb 1985–Nov 1988	46
*NOAA-11***	0230, 1430 LST	Nov 1988–Dec 1992	50

* At launch, *NOAA-9* had equator crossing times at 0220 and 1420 LST.

** At launch, *NOAA-11* had equator crossing times at 0140 and 1340 LST.

Although in principle OLR data would provide an ideal surrogate for tropical convection, the changes in local equatorial crossing time, water vapor window channels, and instruments due to different satellites used from time to time have presented a challenge for using this dataset in climate change studies. In the past, as noted by Chelliah and Arkin (1992), some corrections were made for the changes in water vapor spectral windows and in instruments (Gruber and Krueger 1984), but not for changes in equatorial crossing time among different satellites. When sampling the diurnal cycle at different times, Gadgil et al. (1992) demonstrated that the OLR fluxes in the 1980s as measured by the *NOAA-7* satellite are consistently lower than those in the 1970s, which were measured by the NOAA SR series. They proposed a method for correcting this systematic bias by applying it to the *NOAA-7* data. After bias correction, they found that the OLR variations became consistent with rainfall fluctuations over the Indian region.

A chronology of NOAA satellites, adopted from Chelliah and Arkin (1992), hereafter referred to as CA, is shown in Table 1. As evident from this table, the observation time from the NOAA SR and *6* series is similar but is distinctly different from the other series. CA and, more recently, Kayano et al. (1995) showed that different time of satellite observations is due to either replacement of satellites or long-term drift from orbital planes during the lifetime of single satellites. Another noteworthy feature in Table 1 is that the equatorial crossing time of *TIROS-N* series has shifted by 1 h from *NOAA-7, -9,* and *-11* satellites. Details of corrections are not given here as they are described fully in Gadgil et al. (1992). Suffice to say here that the OLR fluxes from *TIROS-N* and *NOAA-7* to *11* series have

Brought to you by NATIONAL TAIWAN UNIV | Unauthenticated | Downloaded 10/08/23 02:42 PM UTC

been corrected using Eq. (3) as suggested by Gadgil et al. (1992) because of the similar local measurement times among these satellites. The missing OLR data in 1978 (10 months) are filled by the long-term monthly means.

A second dataset used is the tropical cyclone records, which are obtained from the annual tropical cyclone report by the Joint Typhoon Warning Center in Guam. For the Pacific and north Indian Ocean, data are available from 1974 to 1992, but for the south Indian Ocean data are only available since 1981.

3. Methods

Two approaches are adopted here to test trends in the data. The first one relies on simple regression method. Let time (t) be taken as the independent variable, and convection anomaly (Y_t) be the dependent variable. The linear regression model has the following form:

$$Y_t = a + bt + \epsilon_t, \tag{1}$$

where a is the intercept, b the slope, and ϵ_t the residual. Using the least squares method, the slope (i.e., trend) can be estimated as

$$\hat{b} = \frac{\sum_{t=1}^{n} (t - \bar{t})Y_t}{\sum_{t=1}^{n} (t - \bar{t})^2}, \tag{2}$$

where n is the total number of observations, and $\hat{a} = \bar{Y} - b\bar{t}$. Assuming that the residuals are independent and normally distributed with mean zero and variance σ^2, the estimated standard error of b is

$$SE(\hat{b}) = \left[\frac{\sum_{t=1}^{n} (Y_t - \hat{a} - \hat{b}t)^2}{(n-2)\sum_{t=1}^{n} (t - \bar{t})^2} \right]^{1/2}. \tag{3}$$

The goal is to test whether H_0: $b = 0$ based on the fact that $b/SE(b)$ is distributed as Student's t with $n - 2$ degrees of freedom when the null hypothesis (H_0) is true (Woodward and Gray 1993).

The second method to quantify the direction and magnitude of the trend is based on the nonparametric Mann–Kendall rank statistic, τ, where τ is defined as (Kousky and Chu 1978)

$$\tau = 4\,\Sigma m_i/[n(n-1)] - 1, \tag{4}$$

where m_i represents the number of values that are greater than the ith value subsequent to its position in a raw series of n values. Unlike the linear regression method, this test is insensitive to individual outliers and to the start and end points. To apply this statistic to evaluate significance, a comparison is made with

$$\tau_g = \pm t_g[(4n + 10)/\{9n(n-1)\}]^{1/2}, \tag{5}$$

where t_g is the value of t at the given probability level of the Gaussian distribution for a two-tailed test. The use of τ involves ranking and counting of each individual member relative to others in an unranked series. A negative estimate of τ implies a decrease of a variable with time.

4. Assessment of bias-corrected OLR series

CA performed a rotated empirical orthogonal function (REOF) analysis of the uncorrected OLR series over the global Tropics and noted that whereas the first two eigenmodes have a clear physical meaning, the third and fourth modes appear to be related to the changes in the satellite-observing systems. To assess whether the artificial satellite mode depicted in CA's REOF analysis exists in the uncorrected and corrected data as described in section 2, we have performed a REOF analysis of both OLR series over the study domain.

In comparing CA's results with the current study, at least three factors that may contribute to the differences between these two studies should be noted. First, CA used global Tropics as the study domain, while the current study has a more limited domain. Second, the time period used in CA was from 1974 to 1989 and in this study is from 1974 to 1992, and the missing data in 1978 were disregarded in CA. Third, while CA used OLR anomalies, this study uses normalized data in the REOF analysis.

Figure 1 shows the six leading eigenvector patterns of the REOF analysis of the corrected OLR series. Collectively, they explain about 52% of the total variance. The spatial pattern of the first mode (Fig. 1a) depicts a negative center near 130°E and positive anomalies in the equatorial central Pacific. Because of the phase reversal between the central Pacific and western Pacific–eastern Indian Oceans, this pattern represents a mode in which strong (weak) convection over the former region is associated with weak (strong) convection over the latter region. The corresponding time series of the first mode (Fig. 2a) reveals a distinct change of OLR, that is, pronounced excursions of negative anomalies, during the 1982–83, 1986–87, and 1991–92 El Niño–Southern Oscillation (ENSO) episodes. Also noticed is the relative enhancement of ENSO signals in the bias-corrected time series as compared to the uncorrected series. Thus, this pattern may reflect a canonical mode of interannual climate variability associated with an ENSO episode.

For the second eigenmode (Fig. 1b), it also depicts a distinct pair of positive and negative anomalies over the central–western Pacific and the maritime continent, respectively, but the center of anomalies appears to be shifted westward by 10°–20° longitudes relative to the first one (Fig. 1a). The amplitude time series of this mode (Fig. 2b) exhibit large, positive values for some cold-episode years such as 1975, 1984, 1988, and 1989. Again, the fluctuations seem to be generally larger in

Brought to you by NATIONAL TAIWAN UNIV | Unauthenticated | Downloaded 10/08/23 02:42 PM UTC

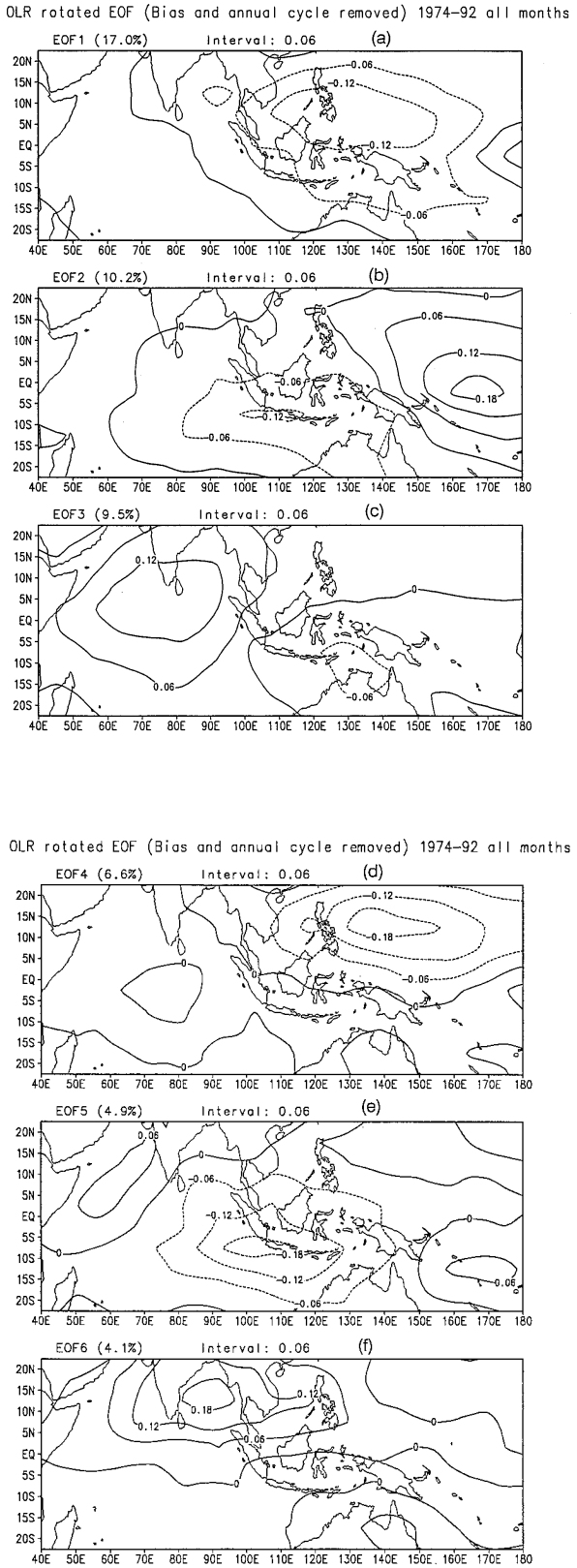

FIG. 1. Spatial patterns of the first six rotated eigenvectors of normalized and bias corrected monthly mean OLR anomalies from June 1974 to December 1992. The contour interval is 0.06.

the corrected series than the uncorrected series. Accordingly, this mode may represent large-scale, tropical OLR features at a different stage of evolution of interannual climate variability.

The spatial pattern of the third mode (Fig. 1c) reveals a contrast between a positive center near the southern tip of India and a small negative center over northern Australia and the adjacent Arafura Sea. This pattern may represent a contrast between the dry Indian Ocean monsoon and the wet Australian summer monsoon during the boreal winter. In Fig. 2c, time series of this mode for both the corrected and uncorrected series show a gradual, long-term downward trend from 1974 to 1992. As will be seen in section 6 (Fig. 3), this long-term change may correspond to a pronounced downward trend found over a large portion of the Indian Ocean as the spatial pattern of this mode is mainly dominated by the positive anomalies over that region (Fig. 1c). Also noted in Figs. 2a–c is the high correlation coefficient between the uncorrected and corrected series for the first three modes (0.79 for the first mode, 0.82 for the second mode, and 0.83 for the third mode).

Broadly similar to the first rotated mode, the spatial pattern of the fourth mode shows a well-organized negative center to the east of the Philippines and positive anomalies over the equatorial central Pacific (Fig. 1d). The spatial structures of the fourth (fifth and sixth too) mode for the corrected and uncorrected data are dissimilar to each other. Temporal variations of the fourth mode of the uncorrected series are very different from those of the corrected series (Fig. 2d). More important, the uncorrected series is marked by two different periods, namely, the period from June 1974 to February 1978 (NOAA SR series) during which the mean of the coefficient is $+0.41$ and the period from April 1983 to December 1992 (*NOAA 7, 9,* and *11*) during which the mean of the coefficient is -0.14. Another noteworthy feature is the abrupt change in the uncorrected time series from late 1981 to early 1982, coinciding with a significant shift in the equatorial crossing times of the satellites from *NOAA 6* to *7* (Table 1). After correction, the fluctuations of the fourth mode become more moderate from late 1981 to early 1982. Interestingly, temporal variations of the corrected series also show ENSO signals in some years (e.g., 1982–83 and 1991–92), and the behavior of this mode is similar to the first mode of the corrected time series (Fig. 2a). Thus, the fourth mode of the uncorrected data seems to be related to the satellite bias and after correction, this mode appears to have a physical meaning.

The spatial pattern of the fifth mode is similar to the second mode although the center of the positive anomalies over the central Pacific associated with the fifth mode is shifted southward to about 15°S (Figs. 1e and 1b). The uncorrected time series of this mode (Fig. 2e) does not exhibit a homogeneous change over a long period of time. After correction, some cold-episode

Brought to you by NATIONAL TAIWAN UNIV | Unauthenticated | Downloaded 10/08/23 02:42 PM UTC

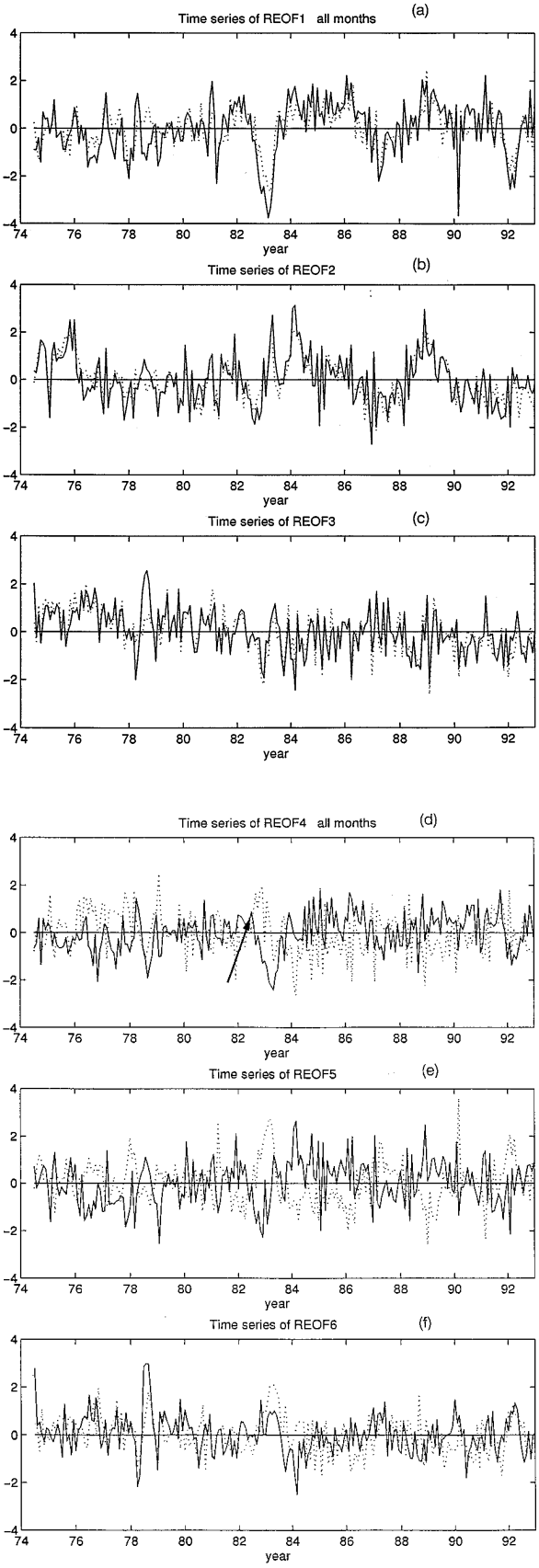

years such as 1984 and 1988–89 stand out more clearly in the time series of coefficients (Fig. 2e).

The sixth rotated mode is characterized by a large, positive center over the Bay of Bengal and its neighboring areas (Fig. 1f); thus, this pattern tends to emphasize variations over the most intense heat source region during the east Asia summer monsoon (Ding 1994). In a way similar to the fourth mode, the uncorrected time series of the sixth mode (Fig. 2f) shows a tendency to be marked by two opposite time periods; that is from June 1974 to February 1978 (NOAA SR series) during which the mean of the coefficient is $+0.35$ and from March 1984 to November 1991 (*NOAA 7, 9,* and *11*) during which the mean of the coefficient is -0.30. Therefore, the fourth and possibly the sixth mode of the uncorrected records appear to be related to the satellite bias. The large spike in 1978 in the corrected time series may not be realistic because the long-term mean values were used to fill the missing gap for the 10 months in 1978 (Fig. 2f).

5. Significance testing of trend patterns

a. Test of trend for local significance under serial correlations

It is well known that geophysical data are temporally correlated; that is, there is persistence in data from time to time. As a consequence, when the test statistic is evaluated for its statistical significance, the number of sample sizes that correspond to the temporal degrees of freedom should be adjusted. One way to determine the ''effective sample size,'' n', is to assume that the underlying data follow a first-order autoregressive process (e.g., Katz 1985). Indeed, first-order autoregressive (or Markov) processes are often found to be good approximations for representing climate time series (e.g., Shukla and Mo 1983). Given the lag-one autocorrelation coefficient, ρ_1, the ''effective sample size'' can be estimated as

$$n' \approx n \frac{1 - \rho_1}{1 + \rho_1}. \tag{6}$$

After temporal degrees of freedom are properly adjusted, the estimated trends at each grid point are individually tested for significance at the 95% level.

b. Tests of trend for field significance

The aforementioned method is applied for individual locations within the field. However, because of the spatial interdependence of the individual OLR measurements, it is also necessary to address the collective sig-

FIG. 2. Amplitude time series corresponding to the first six rotated modes of the spatial patterns from the corrected OLR data (solid line) and uncorrected data (dotted line).

Brought to you by NATIONAL TAIWAN UNIV | Unauthenticated | Downloaded 10/08/23 02:42 PM UTC

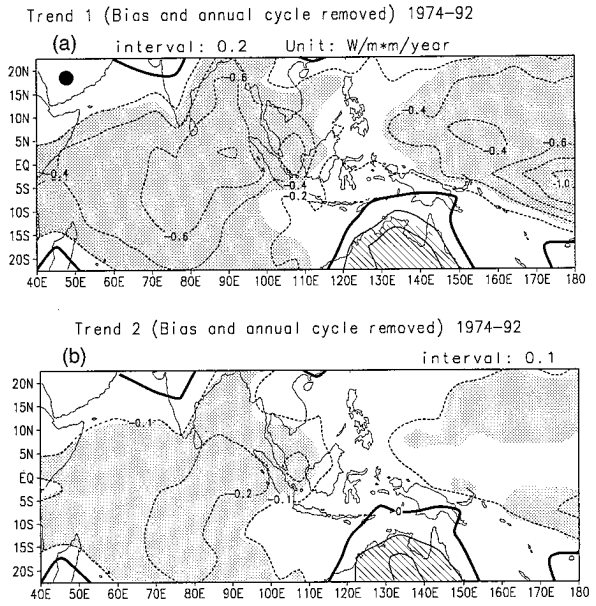

FIG. 3. Contour plots of (a) the linear OLR trends in W m^{-2} yr^{-1} and (b) the Mann–Kendall rank statistic of OLR from June 1974 to December 1992. Thin solid line denotes positive trend and thin dashed line denotes negative trend. Heavy solid line denotes zero trend. Hatching and stippling mark regions where trends are locally significant at the 95% level. A solid circle in the upper-left corner of (a) indicates 95% ''field significance'' through Monte Carlo testing when spatial coherence is taken into account. No analysis has been done for Saudi Arabia because of its extreme aridity.

nificance of a finite set of individual significance tests for the entire field. Assume that N out of the entire M grid points in the study domain reach the local significance at the 95% confidence level from a simple regression analysis. A natural question is whether this pattern could have occurred by chance. At this specified level, 5% of M grid points might be expected to be significant by chance even if the true slope were zero. If the actual number of total grid points showing local significance (N) exceeds that by random chance, as a first guess, the spatial pattern may be considered field significant. However, because of the spatial correlation in OLR data, in reality, the percentage of the field showing significant results should be far greater than that by chance. As will be seen later, this is the case here.

A more rigorous test to assess the statistical significance of trend is by Monte Carlo simulations. Time series of monthly mean OLR series (i.e., 223 months for the entire period, 112 months for summer, or 111 months for winter) at each grid point (280 grids) for the period from 1974 to 1992 are ''concurrently'' shuffled using a random number generator. A linear regression slope is estimated at each grid point; the total number of grids showing significance at the 95% confidence level is counted and denoted as N^i_{mc}, where the superscript i denotes the ith trial and the subscript mc denotes the Monte Carlo experiments. When the procedures for a large number of trials (500 times) are repeated, the field is considered to be significant at the 95% level when N exceeds N^*_{mc}, where N^*_{mc} is the 95 percentile of a locally significant trend from 500 trials. It is recognized that the above resampling procedure, while preserving spatial correlation, may scramble time ordering of individual data points. This has been cautioned most recently by Wilks (1997).

6. Trend analyses

a. Complete duration time series

Figure 3a shows the estimated linear slope of OLR for the entire, consecutive 223 months from 1974 to 1992 using (2). A large area of negative and statistically significant slope, indicative of an increasing trend in convection, is found over the tropical western–central Pacific Ocean, with the largest slope values being in the equatorial south-central Pacific near the date line. The change over a large portion of the Indian Ocean and the South China Sea appears to be in phase with that over the western–central Pacific. Positive OLR slopes, possibly indicative of reduced tropical convection over time, are noted over northwestern India, southern Madagascar, southern New Guinea and tropical Australia where the largest values are noted.

As variations in OLR are not only caused by clouds, the positive slopes of OLR over Australia probably reflect a change of surface temperature in this region and should not be interpreted as a decrease in convection (Chou 1994). Another possibility for the large slope over Australia may be due to the fact that the formula used for correcting bias as discussed previously in section 2 is a universal one for all tropical oceans; it may not be appropriate for the large, arid, or semi-arid regions such as Australia where the diurnal cycle in surface temperature is very pronounced (CA; Kayano et al. 1995). Therefore, caution must be exercized for interpreting trends in the tropical convection and rainfall over large, arid land regions even after satellite biases due to changes in observation time have been universally corrected.

As a complement to Fig. 3a, Fig. 3b displays the OLR trend based on the Mann–Kendall rank statistic. It is basically in agreement with the results from the simple linear regression analysis, in likewise showing negative values over a large portion of the central and western Pacific Ocean and the Indian Ocean, and positive estimates over tropical Australia, northwest India, and southern Madagascar. Compared with Fig. 3a, the area of negative and locally significant trends of OLR in the western/central Pacific is reduced in Fig. 3b.

b. Northern summer

Because the area of interest is located in the monsoon area where the seasonal change in wind, convection, and rainfall is conspicuous (e.g., India summer mon-

Brought to you by NATIONAL TAIWAN UNIV | Unauthenticated | Downloaded 10/08/23 02:42 PM UTC

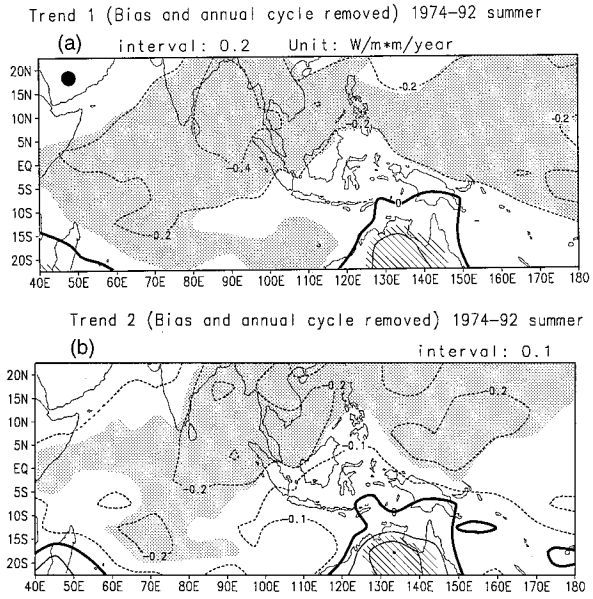

FIG. 4. Same as in Fig. 3 except for the boreal summer (April–September).

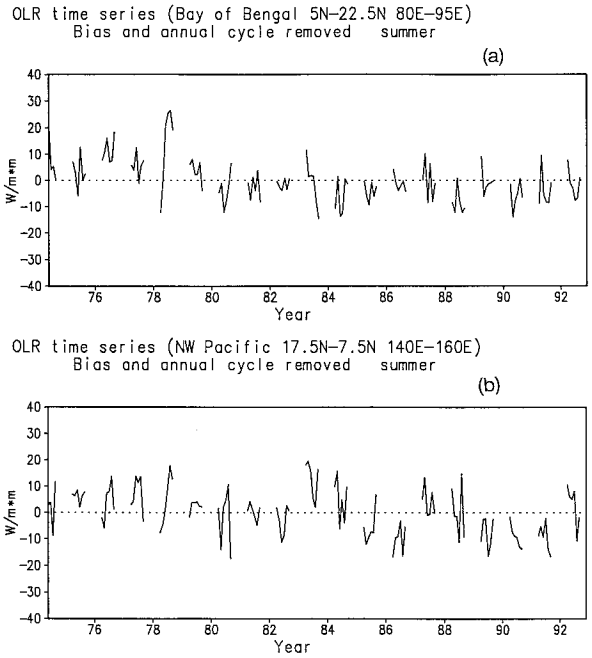

FIG. 5. Time series of the area-averaged OLR records in (a) Bay of Bengal and (b) northwest Pacific for the boreal summer (April–September).

soon), it is also instructive to know temporal variations of tropical convection when data are partitioned into summer and winter half-years. Unless otherwise stated, the Northern Hemispheric season is adopted and summer is defined as the six-month period from April to September; winter is referred to as the other six-month period from October to March. The six-month time gap, say, between October of one year and March of the next year, is taken into account by properly incrementing the time variable.

Figure 4a displays the linear regression slope of OLR during summer. Negative and locally significant slopes (increased convection) are found mainly over the Northern Hemisphere in a large patch extending eastward from the Arabian Sea, India, the Bay of Bengal, southeast Asia including the South China Sea, to the northwest Pacific. Positive and statistically significant slopes prevail over a large portion of northern Australia, as also shown in Fig. 4b.

To further illustrate the temporal variation of convection, Fig. 5 shows the time series plot of the area-averaged summer OLR for the Bay of Bengal and the western North Pacific. A downward trend in OLR is clearly evident in both series. Over the last 19 yr, the decrease in OLR as judged from the simple regression analysis is about 11 and 8 W m^{-2} for the Bay of Bengal and the northwest Pacific, respectively. As summer is the rainy season in Asian monsoon regions, the increased convection revealed in Figs. 4 and 5 implies a tendency for increased summer monsoon rainfall.

c. Northern winter

For the winter half-year, Fig. 6a features a downward and locally significant slope in the equatorial south-central Pacific and a large portion of the south-central Indian Ocean and a significant upward slope over Molucca Sea, southeastern Australia, and to the east of New Caledonia. The increase in convection over the equatorial south-central Pacific and the south-central Indian Ocean is also reflected in the nonparametric test in Fig.

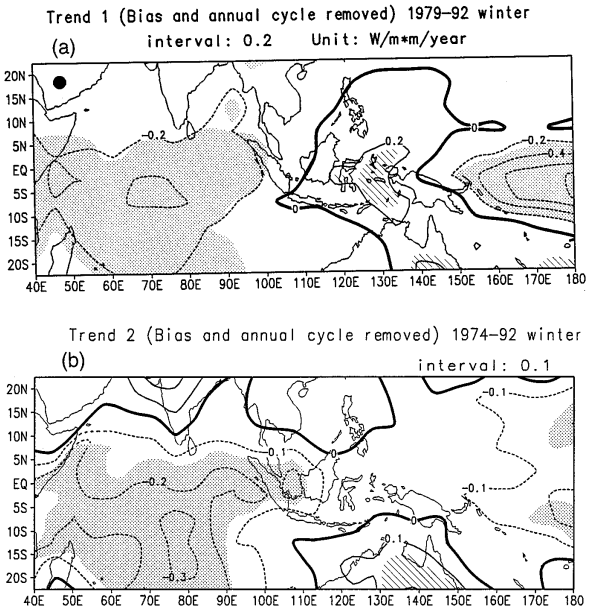

FIG. 6. Same as in Fig. 3 except for the boreal winter (October–March).

Brought to you by NATIONAL TAIWAN UNIV | Unauthenticated | Downloaded 10/08/23 02:42 PM UTC

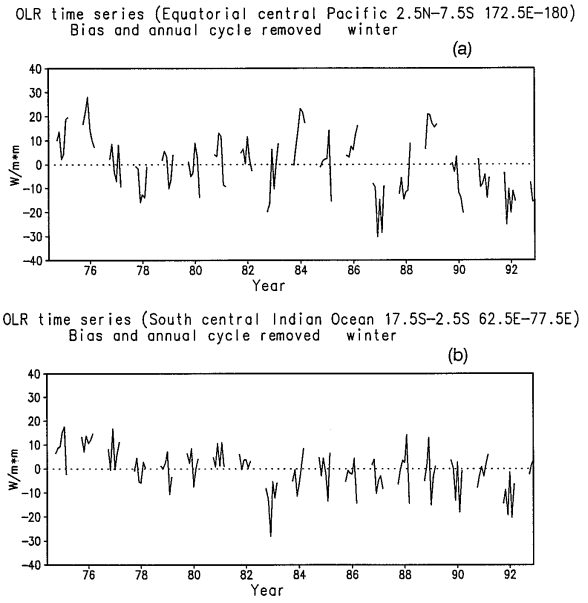

FIG. 7. Time series of the area-averaged OLR records in (a) equatorial south-central Pacific and (b) south-central Indian Ocean for the boreal winter (October–March).

6b and in the time series plots in Fig. 7. Over the entire 19-yr period, the decrease in OLR is approximately 15 W m^{-2} over the south-central Pacific and 11 W m^{-2} over the south-central Indian Ocean.

At the peak of the austral summer, the monsoon trough is located near the north of Australia, bringing monsoon rains to the extensive region of Sumatra, Java, tropical Australia, Papua-New Guinea, and the southwest Pacific. This wet season is distinguished from the austral winter when tropical Australia is marked by a dry season. Therefore, a positive slope in OLR suggests either a weaker Australian summer monsoon over the past 19 yr or the universal formula proposed by Gadgil et al. (1992) does not effectively remove the bias over large semiarid tropical land regions where the diurnal surface heating is strong. Likewise, the positive slope over India does not necessarily imply a decrease in convection in the winter season as India is under the influence of the prevailing dry northeasterlies.

d. Time history of tropical cyclones

In previous sections, increased convection is noted in the Bay of Bengal, the south-central Indian Ocean, and the northwestern Pacific Ocean in their respective summers. Because tropical cyclones are intense convection systems and are formed over warm waters, a natural question arises as to whether there is any appreciable change in the number of tropical cyclones associated with changes in convection as inferred from the OLR series. Figure 8 shows the concurrent time series of cyclone counts for these three regions. The straight line denoting the linear regression line is only used for il-

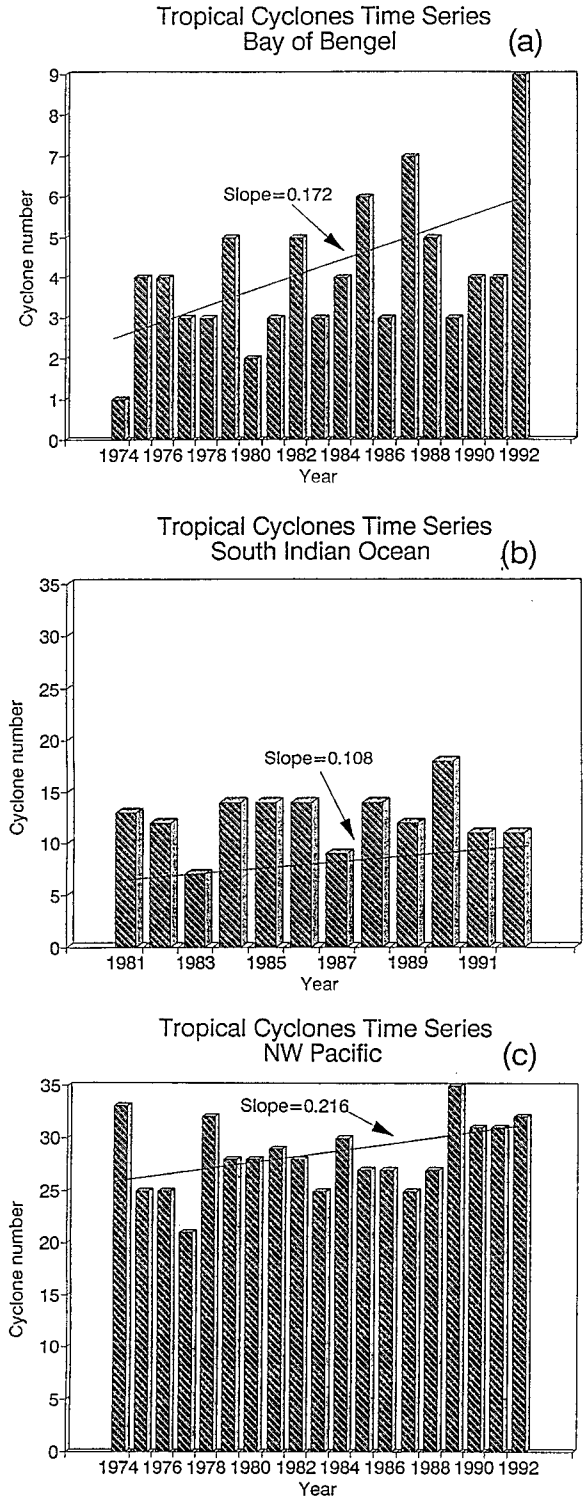

FIG. 8. Time series of the number of tropical cyclones in (a) Bay of Bengal, (b) South Indian Ocean, and (c) northwest Pacific. For illustrative purpose, straight line denotes the linear regression line and the unit for slope is number of cyclones per year. Note that the vertical scale used in (a) is different from (b) and (c).

Brought to you by NATIONAL TAIWAN UNIV | Unauthenticated | Downloaded 10/08/23 02:42 PM UTC

lustrative purpose. A general upward trend is found in all three regions, which is consistent with the increased convection in Figs. 4–7. It is recognized that fitting a specific counting distribution to the annual number of tropical cyclones might be more appropriate (Solow and Nicholls 1990). However, this would require developing a statistical model for each region and is thus beyond the scope of the current study.

7. Sensitivity analyses

a. Effects of ENSO

The results presented in the preceding section refer to the conditions when ENSO events are included in the trend analyses. Because the interannual variability of convection and rainfall in the tropical Pacific and the Indian Ocean is intimately related to the recurring ENSO phenomenon (e.g., Lau and Sheu 1991; Rasmusson 1991), it is of utmost interest to examine the temporal variations of tropical convection when the short-term climate variability such as ENSO is removed from the analyses. For this purpose, the following ENSO year pairs comprising 1976–77, 1982–83, 1986–87, and 1991–92, are excluded. Because the results from the Mann–Kendall statistic are similar to those from the regression approach, only the results from the latter will be presented.

Figure 9a displays the OLR linear trend when the ENSO years are absent. There are features common to Figs. 9a and 3a: negative slopes occur over the tropical western Pacific, southeast Asia including the South China Sea, the Bay of Bengal, the Arabian Sea, and the south Indian Ocean, and positive slopes occur over Australia and southern Madagascar (note that the intervals used in Fig. 9a are twice those of Fig. 3a). However, the large decrease over the equatorial south-central Pacific seen in Fig. 3a gives way to a smaller decrease when ENSO years are removed from the analysis (Fig. 9a). This is understood as follows. At the height of an ENSO event, warm pools of seawater and the attendant convection generally shift eastward to the equatorial central Pacific. This eastward displacement of convection reinforces the preexisting one over the south-central Pacific and results in a well-organized pattern of enhanced convection as seen in Fig. 3a. Without ENSO, tropical convection over the equatorial central Pacific is thus expected to be weaker.

For the boreal summer, Fig. 9b shows large areas of the significantly negative slopes in the Northern Hemisphere, extending eastward from the eastern tip of the Arabian Sea, India, the Bay of Bengal, a large part of Indochina, and the South China Sea to the northwestern Pacific, with a branch extending from northern New Guinea southeastward to the Coral Sea. A comparison between Figs. 9b and 4a indicates that an increase in convection is unabated in a swath extending from the Bay of Bengal across the South China Sea to the northwestern Pacific if the ENSO years are not retained in the analysis.

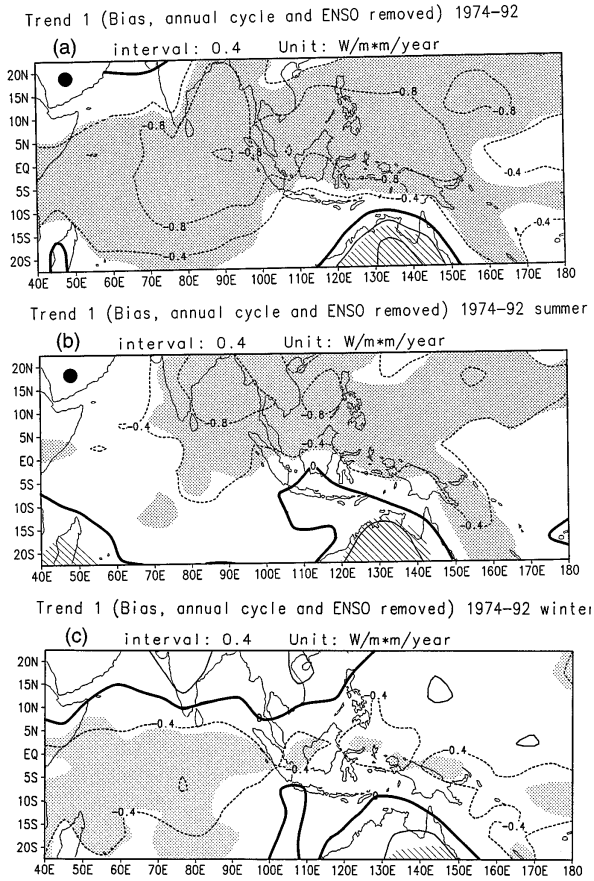

FIG. 9. Contour plots of the linear OLR trends in W m^{-2} yr^{-1} from 1974 to 1992, excluding 1976–77, 1982–83, 1986–87, and 1991–92: (a) all seasons, (b) boreal summer, and (c) boreal winter. Symbols as in Fig. 3a.

During the boreal winter without ENSO years (Fig. 9c), negative and statistically significant slopes cover primarily the South Indian Ocean, and positive slopes still dominate Australia.

b. Effects of endpoint values

It is recognized that trends detected from the linear regression method might be sensitive to the values at the start and end points in the time series. To test how sensitive the results are to the different end points, we vary the data length from 1974–92 to two different periods, that is, 1974–90 and 1979–92. Figures 10a and 10b show the linear trend estimated from these two different data periods. Again, the most conspicuous features are the large, negative, and statistically significant OLR slopes over the equatorial south-central Pacific, the northwest Pacific, and the Bay of Bengal and the equatorial Indian Ocean. Likewise, large, positive slopes are still found over Australia. In fact, the patterns re-

Brought to you by NATIONAL TAIWAN UNIV | Unauthenticated | Downloaded 10/08/23 02:42 PM UTC

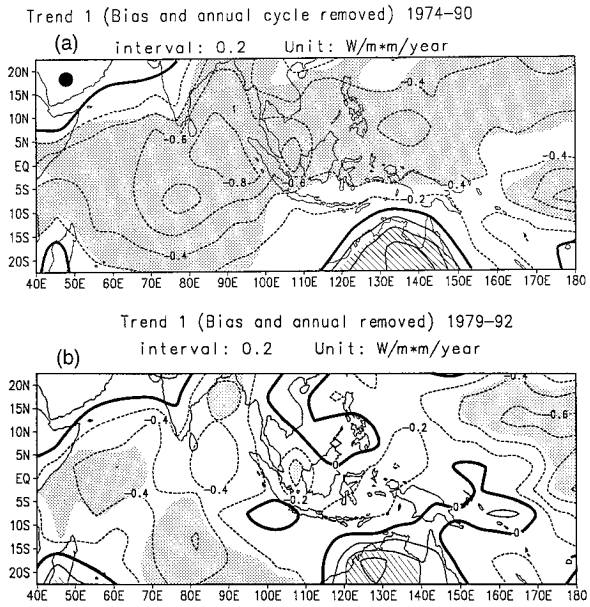

FIG. 10. Same as in Fig. 3a except the data length is shortened to (a) 1974–90 and (b) 1979–92.

vealed in Fig. 10a are very similar to that in Fig. 3a. However, when the 1974–78 period is excluded from the analysis (Fig. 10b), the change in sign is reversed in some regions (e.g., a portion of the South China Sea) as compared to the patterns shown in Fig. 3a. Thus, when the period for the NOAA SR series is disregarded, some changes occur over the regions where the trend values are relatively small in the entire data record, although the major features seen in Fig. 3a are preserved.

c. Effects of missing observations

Furthermore, because the missing 10 months in 1978 were filled by the long-term monthly mean values, there is some concern whether this filling has changed the resulting trend pattern as seen in Fig. 3a. In this regard, we have also produced another diagram by eliminating these 10 months from the time series. Results from this new series (not shown), however, do not show any apparent differences from Fig. 3a, in which the missing 10 months had been filled.

8. Summary and discussion

In this study, the uncorrected and corrected OLR datasets have been subjected to the rotated EOF analysis separately and a bias due to changes in equatorial crossing time among various satellites is identified in the uncorrected data. A comparison of the REOF modes between the uncorrected and corrected data indicates that the satellite bias, to a first approximation, has been corrected. Simple linear and nonparametric trend analyses are then used independently to determine whether there is any climate change in convection, as inferred from the corrected OLR dataset, over the tropical Indian and western–central Pacific Ocean regions. For the period June 1974 to December 1992, results indicate that a negative slope in OLR series (an increase in convection) in the tropical central–western Pacific appears to be in phase with that in the Indian Ocean (Fig. 3). Meantime, tropical Australia experienced a positive slope.

When the data are broken into summer and winter half-years, an increase in convection shows a preference to occur in the summer hemisphere. During the boreal summer (Fig. 4), increase in convection occurs mainly over India, the Bay of Bengal, southeast Asia, and the northwestern Pacific. Time series of tropical cyclone counts in the Bay of Bengal and northwest Pacific indicate a general level of increase and support independently the results revealed from OLR analyses. During the austral summer (Fig. 6), increase in convection is more confined in the Southern Oceans over the central Pacific and the Indian Ocean. Unaffected by the seasonality, a large portion of tropical Australia is always characterized by a positive slope in OLR.

If ENSO years are removed from the data, the broad-scale pattern of the linear trend is very similar to that when they are not removed although the magnitude of the trend is changed. For summer (Fig. 9b), the enhancement of convection is shown over the northwest Pacific, the South China Sea, southeast Asia, the Bay of Bengal, and India. For winter (Fig. 9c), the most noteworthy features include an increase of convection with time over the south Indian Ocean and a few small patches over the south-central and equatorial western Pacific.

In analyzing both long-term surface rainfall and high-level cloud amount records from geostationary meteorological satellites, Nitta and Kachi (1994) noted an increase in rainfall in the tropical central Pacific and the eastern extreme of the south Indian Ocean from the mid 1970s to the 1980s, but a decrease in rainfall in the western Pacific over the same time period. They attributed these decadal-scale rainfall changes to gradual alterations in sea surface temperatures brought about by the recurring ENSO phenomena that prevailed in the tropical Pacific during recent decades. Graham (1994) studied decadal-scale, boreal winter circulation in the Pacific using observations, and numerical model outputs. He found an eastward displacement of the region of enhanced convection and SST in the Pacific from 1970 to 1982 and attributed this change to a shift in background mean state. Interestingly, Wang (1995) also noted that SST variations over the tropical Pacific and the Indian Ocean have exhibited both ENSO (interannual) and interdecadal timescales. Applying a filter that is equivalent to 7-yr running mean to suppress the ENSO mode, Wang showed a rapid transition from the cold to the warm state in the late 1970s and such a warm state remained thereafter in the interdecadal mode.

Brought to you by NATIONAL TAIWAN UNIV | Unauthenticated | Downloaded 10/08/23 02:42 PM UTC

This warm interdecadal mode in SST would fuel the overlying atmosphere with additional warmth and moisture, reduce the atmospheric static stability, and increase the likelihood of moist convection. Therefore, the general level of increase in convection seen in this study is probably inherently coupled to the decadal-scale tropical Pacific Ocean warming detected by Nitta and Yamada, Graham, Wang, and others. It is plausible that the increase in convection observed over the western Pacific and Indian Ocean in this study need not be an ENSO-related phenomenon as suggested by Nitta and Kachi (1994) because this signal is also present in the dataset without ENSO years. Rather, it can be interpreted as a change in the climate mean state involving a coupling of tropical ocean and atmosphere in the monsoon area with a decadal timescale.

Acknowledgments. This study is partially supported by the UH-EWC collaborative research program. PSC benefitted from Rick Katz's reading of the draft. We thank the anonymous reviewers and Gene Rasmusson for comments that were very helpful in improving the original version of this paper.

REFERENCES

Chelliah, M., and P. Arkin, 1992: Large-scale interannual variability of monthly outgoing longwave radiation anomalies over the global tropics. *J. Climate,* **5,** 371–389.

Chou, M.-D., 1994: Coolness in the tropical Pacific during an El Niño episode. *J. Climate,* **7,** 1684–1692.

Ding, Y., 1994: *Monsoon over China.* Kluwer Academic Publishers, 419 pp.

Gadgil, S., A. Guruprasad, and J. Srinivasan, 1992: Systematic bias in the NOAA outgoing longwave radiation dataset? *J. Climate,* **5,** 867–875.

Gladwell, J. S., and M. Bonell, 1990: An international programme for environmentally sound hydrologic and water management strategies in the humid tropics. *Symp. Tropical Hydrology,* San Juan, Puerto Rico, UNESCO, 10 pp.

Graham, N. E., 1994: Decadal-scale climate variability in the tropical and North Pacific during the 1970s and 1980s: Observations and model results. *Climate Dyn.,* **10,** 135–162.

Gruber, A., and A. F. Krueger, 1984: The status of the NOAA outgoing longwave radiation dataset. *Bull. Amer. Meteor. Soc.,* **65,** 958–962.

Katz, R. W., 1985: Probabilistic models. *Probability, Statistics, and Decision Making in the Atmospheric Sciences,* A. H. Murphy and R. W. Katz, Eds., Westview, 261–288.

Kayano, M. T., V. E. Kousky, and J. E. Janowiak, 1995: Outgoing longwave radiation biases and their impacts on empirical orthogonal function modes of interannual variability in the Tropics. *J. Geophys. Res.,* **100** (D2), 3173–3180.

Kousky, V. E., and P.-S. Chu, 1978: Fluctuations in annual rainfall for northeast Brazil. *J. Meteor. Soc. Japan,* **56,** 457–465.

Krishnamurti, T. N., and N. Surgi, 1987: Observational aspects of summer monsoon. *Monsoon Meteorology,* C.-P. Chang and T. N. Krishnamurti, Eds., Oxford University Press, 3–25.

Lau, K.-M., and C.-P. Chang, 1987: Planetary scale aspects of the winter monsoon and atmospheric teleconnections. *Monsoon Meteorology,* C.-P. Chang and T. N. Krishnamurti, Eds., Oxford University Press, 161–202.

——, and P. J. Sheu, 1991: Teleconnections in global rainfall anomalies: Seasonal to inter-decadal time scales. *Teleconnections Linking Worldwide Climate Anomalies,* M. H. Glantz, R. W. Katz, and N. Nicholls, Eds., Cambridge University Press, 227–256.

Motell, C. E., and B. C. Weare, 1987: Estimating tropical Pacific rainfall using digital satellite data. *J. Climate Appl. Meteor.,* **26,** 1436–1446.

Nitta, T., and S. Yamada, 1989: Recent warming of tropical sea surface temperature and its relationship to the Northern Hemisphere circulation. *J. Meteor. Soc. Japan,* **67,** 375–382.

——, and M. Kachi, 1994: Interdecadal variations of precipitation over the tropical Pacific and Indian Oceans. *J. Meteor. Soc. Japan,* **72,** 823–831.

Palmer, T. N., and D. A. Mansfield, 1984: Response of two atmospheric general circulation models to sea-surface temperature anomalies in the tropical east and west Pacific. *Nature,* **310,** 483–485.

Rasmusson, E. M., 1991: Observational aspects of ENSO cycle teleconnections. *Teleconnections Linking Worldwide Climate Anomalies,* M. H. Glantz, R. W. Katz, and N. Nicholls, Eds., Cambridge University Press, 309–343.

Shukla, J., and K. C. Mo, 1983: Seasonal and geographical variation of blocking. *Mon. Wea. Rev.,* **111,** 388–402.

Solow, A., and N. Nicholls, 1990: The relationship between the Southern Oscillation and tropical cyclone frequency in the Australian region. *J. Climate,* **3,** 1097–1101.

Wang, B., 1995: Interdecadal changes in El Niño onset in the last four decades. *J. Climate,* **8,** 267–285.

Wilks, D. S., 1997: Resampling hypothesis tests for autocorrelated fields. *J. Climate,* **10,** 65–82.

Woodward, W. A., and H. L. Gray, 1993: Global warming and the problem of testing for trend in time series data. *J. Climate,* **6,** 953–962.

Yoo, J.-M., and J. A. Carton, 1988: Outgoing longwave radiation derived rainfall in the tropical Atlantic, with emphasis on 1983–84. *J. Climate,* **1,** 1047–1054.

Brought to you by NATIONAL TAIWAN UNIV | Unauthenticated | Downloaded 10/08/23 02:42 PM UTC